JGR Earth Surface

RESEARCH ARTICLE
10.1029/2018JF004908

Key Points:
- We develop a model to quantify the magnitude of changes in past sediment delivery to prograding coasts based on beach-ridge morphology
- We validate the model against a field site with a history of beach and ridge growth and then apply it to a prehistorically developed site
- The model is most applicable to investigations of coastal evolution with limited geochronologic control

Supporting Information:
- Supporting Information S1
- Table S1
- Table S2
- Table S3
- Table S4

Correspondence to:
D. J. Ciarletta,
ciarlettad1@montclair.edu

Citation:
Ciarletta, D. J., Shawler, J. L., Tenebruso, C., Hein, C. J., & Lorenzo-Trueba, J. (2019). Reconstructing coastal sediment budgets from beach- and foredune-ridge morphology: A coupled field and modeling approach. *Journal of Geophysical Research: Earth Surface*, *124*, 1398–1416. https://doi.org/10.1029/2018JF004908

Received 5 OCT 2018
Accepted 21 APR 2019
Accepted article online 29 APR 2019
Published online 5 JUN 2019

Reconstructing Coastal Sediment Budgets From Beach- and Foredune-Ridge Morphology: A Coupled Field and Modeling Approach

Daniel J. Ciarletta[1], Justin L. Shawler[2], Christopher Tenebruso[1], Christopher J. Hein[2], and Jorge Lorenzo-Trueba[1]

[1]Department of Earth and Environmental Studies, Montclair State University, Montclair, NJ, USA, [2]Virginia Institute of Marine Science, William & Mary, Gloucester Point, VA, USA

Abstract Preserved beach and foredune ridges may serve as proxies for coastal change, reflecting alterations in sea level, wave energy, or past sediment fluxes. In particular, time-varying shoreface sediment budgets have been inferred from the relative size of foredune ridges through application of radiocarbon and optically stimulated luminescence dating to these systems over the last decades. However, geochronological control requires extensive field investigation and analysis. Purely field-based studies might also overlook relationships between the mechanics of sediment delivery to the shoreface and foredune ridges, missing insights about sensitivity to changes in sediment budget. We therefore propose a simple geomorphic model of beach/foredune-ridge and swale morphology to quantify the magnitude of changes in cross-shore sediment budget, employing field measurements of ridge volume, ridge spacing, elevation, and shoreline progradation. Model behaviors are constrained by the partitioning of sediment fluxes to the shoreface and foredune ridge and can be used to reproduce several cross-shore patterns observed in nature. These include regularly spaced ridges ("washboards"), large singular ridges, and wide swales with poorly developed ridges. We evaluate our model against well-preserved ridge and swale systems at two sites along the Virginia Eastern Shore (USA): Fishing Point, for which historical records provide a detailed history of shoreline progradation and ridge growth, and Parramore Island, for which a relatively more complex morphology developed over a poorly constrained period of prehistoric growth. Our results suggest this new model could be used to infer the sensitivity of field sites across the globe to variations in sediment delivery.

Plain Language Summary Understanding past change in the sediment budgets of coastal systems is expensive and time consuming, often missing crucial insights about sensitivity to future changes. In this study, we developed a model to reconstruct sediment delivery through time, using relationships describing the size and distribution of beach ridges relative to rate of shoreline advance. We tested our model against a field site with a detailed history of coastal evolution, later applying it to a location which largely developed in a prehistoric setting. Our results show that we can use field and remote measurements of beach ridges to model past rates of sediment delivery, providing insights into how future changes may affect the behavior of coastal systems.

1. Introduction

Coastal ridge and swale systems, composed predominantly of relict wave-built beach ridges and/or aeolian foredune ridges, are found in association with progradational shorelines around the world (Tamura, 2012). The morphology of these elongate, shore-parallel to subparallel features preserve paleoenvironmental signatures which have been used to infer changes in shoreline position (Mason, 1993), coastal sediment delivery rates and textures (Bristow & Pucillo, 2006; Hein et al., 2016), relative sea level (Billy et al., 2015; Hede et al., 2013; Long et al., 2012), and storm frequency (Buynevich et al., 2004; Costas et al., 2016). Subsequently, ridge proxies could be useful in predicting future changes to the coastal zone in response to autogenic forcings, climate change, and anthropogenic interventions.

The morphology of relict beach/foredune ridges have been used to infer changes in shoreline migration for at least a century (Johnson, 1919). However, whereas modern studies employing historical mapping, beach profiling, lidar investigations, and shallow stratigraphy provide insight into the scales and sediment budget contributions of various short-term shoreline processes (Dougherty et al., 2016; Pye & Blott, 2016; Saye et al.,

2005; Young & Ashford, 2006), quantifying long-term changes in sediment flux across the Holocene has been constrained by the need for geochronologic control.

Studies of prehistoric spatiotemporal change in regressive coastal systems commonly rely on a combination of radiocarbon dating and optically stimulated luminescence (OSL) to derive geochronology (e.g., Argyilan et al., 2010; Hails, 1968; Oliver et al., 2015; Rhodes, 1980; Rink & Forrest, 2005). Both techniques can be combined with high-resolution topography (i.e., derived from lidar or real-time kinematic GPS mapping), ground-penetrating radar (e.g., Dougherty et al., 2016; Oliver, Donaldson, et al., 2017), and sediment coring to produce quantitative analyses of sediment flux at a given field site. However, these approaches are both expensive and time and labor intensive.

In contrast, quantitative models of geomorphic change, grounded in field-based conceptual models of site evolution, present an opportunity for a more rapid and cost-effective approach to reconstructing time-varying controls of coastal change. We use simple geomorphic relationships, combined with minimal age control points, to develop a morphological model that applies a cross-shore mass balance approach to an idealized ridge and swale morphology in order to quantify past changes in sediment budget. Application of this model to several test field sites provides insight on the sensitivity of coastal systems to variations in sediment delivery. As a tool, the model could be used to explore how changes in sediment fluxes and accommodation (e.g., sea level rise or fall) might impact future shoreline response.

For this study, we initially consider ridge and swale systems composed of shore-parallel relict foredunes and evaluate our model at two sites along the Eastern Shore of Virginia (USA; Figure 1). One site, Fishing Point (an elongating barrier spit at the southern end of Assateague Island), formed in historical times and allows for the construction of a time series analysis of sediment inputs (Table 2) based on observations from aerial photos and recent lidar data. The other site, Parramore Island, features a prominent ridge and swale system that formed during a period of prehistoric progradation. We validate our model framework at Fishing Point using the short-term time series, demonstrating that we can quantify the magnitude of past sediment fluxes from morphology. We later apply the model to Parramore Island, where no time series data exist and only limited chronological control is available.

2. Background: Development of Beach and Foredune-Ridge Systems

While it has not before been directly parameterized, a widely observed morphologic characteristic of ridge and swale systems is the systematic spacing of foredune ridges. Nucleation of incipient foredunes along prograding shorelines occurs through a range of processes (Hesp, 2011; Otvos, 2000) but in many cases is observed to produce a regular pattern of ridge spacing and height (Figure 2). In describing the process driving this periodicity, Johnson (1919) observed that wave-formed platforms could act as regular anchor points for aeolian accumulation, a process later termed "berm-ridge progradation" (Otvos, 2000). Under this process, aeolian-capped, wave-built beach ridges episodically develop upon a substrate provided by the welding of nearshore bars, this process typically associated with inlet sediment bypassing along prograding barrier islands and river mouth strandplain systems (FitzGerald, 1984; Nooren et al., 2017).

For barrier islands, nearshore bars—specifically, elongated inlet attachment bars—taper downdrift from ebb tidal deltas, moving onshore as large packages of sediment with lengths of 300–1,500 m and widths of 40–300 m (FitzGerald, 1982). As a bar moves up the shoreface, it is subject to increasing subaerial exposure during the tidal cycle, which slows its rate of landward advance and contributes to the production of a swale between the bar and the beach, forming a ridge and runnel-like system—although FitzGerald (1982) emphasizes that these systems are much larger than true ridges and runnels and form over longer timescales. Such quasi-cyclic welding of nearshore bars is widely recognized and occurs on the order of every 4–7 years (Price Inlet, South Carolina; FitzGerald, 1984) to 8 years (Skallingen, Denmark; Aagaard et al., 2004) but may be more or less frequent.

While welding events can trigger new ridge formation, the location of an incipient foredune ridge relative to the shoreline is controlled by the influence of waves and the salt tolerance of pioneering plants, which help stabilize the incipient foredune (Vinent & Moore, 2013). This shoreline setback has been theorized to relate to the cross-shore gradient in plant community that occurs on the beach, with narrower zonation (inversely

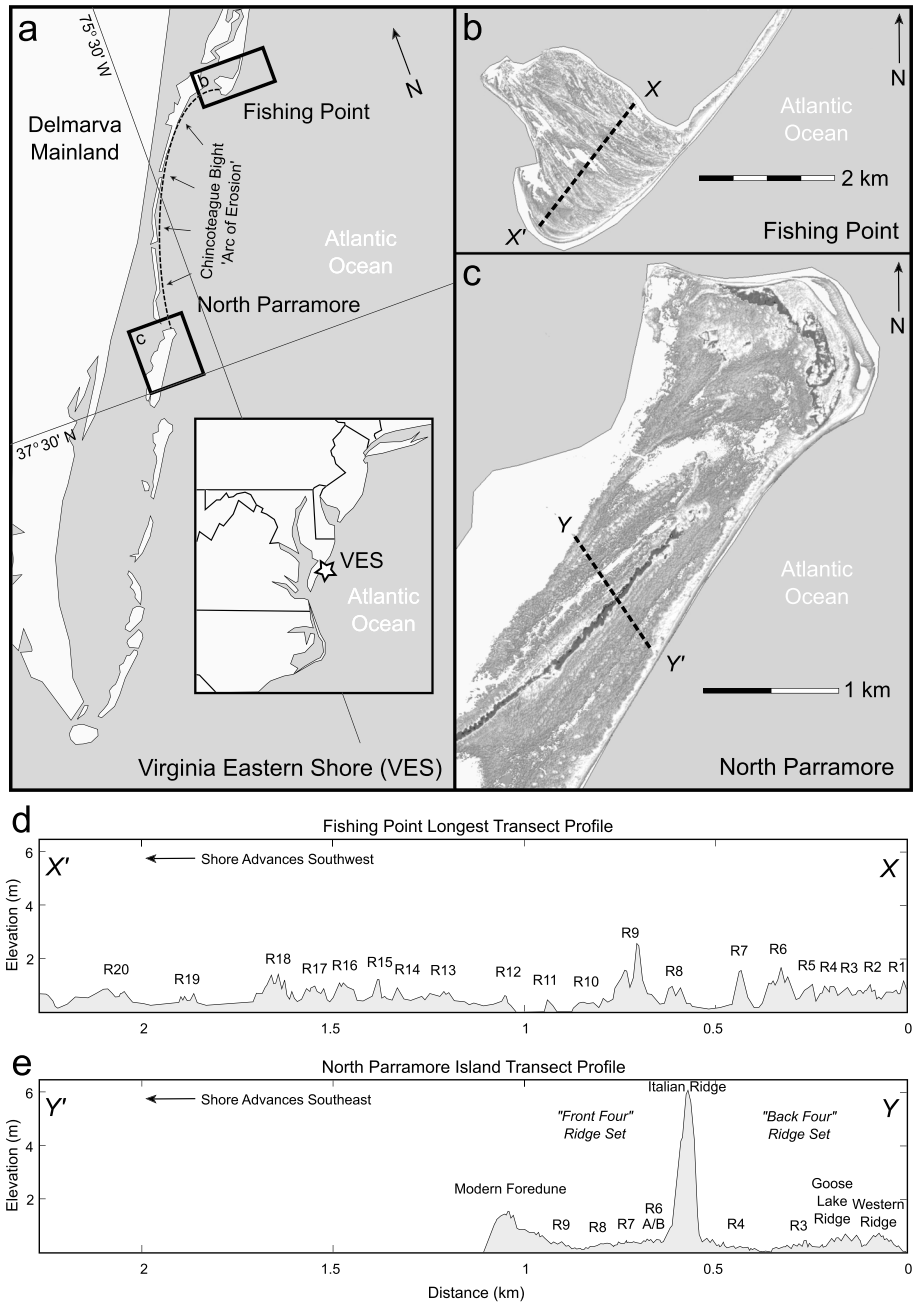

Figure 1. (a) Map overview of the Virginia Eastern Shore (VES), at the southern end of the Delmarva Peninsula on the U.S. Atlantic coast. (b) Hillshaded lidar-derived digital elevation models of Fishing Point and (c) North Parramore Island, showing orientation of ridge and swale systems. Highest elevations on Fishing Point are >3 m, while some points on North Parramore reach >7 m above mean higher high water. (d) Ridge-perpendicular transects of Fishing Point and (e) Parramore Island showing elevation profiles referenced to mean higher high water. Individual ridges are numbered from landward to seaward, unless otherwise named.

proportional to wave height, since this acts as a disturbance factor) leading to more stable, linear foredune ridges capable of producing consistent patterns of ridge height and spacing.

Modeling suggests that the height of purely aeolian foredunes could reflect a steady state condition associated with the local sediment supply regime and the presence/absence of stabilizing vegetation (Vinent & Moore, 2013). More recently, it has been shown that dune height is primarily a function of sediment supply, whereby vertical growth rate responds strictly to the size of the ridge (Davidson-Arnott et al., 2018). For

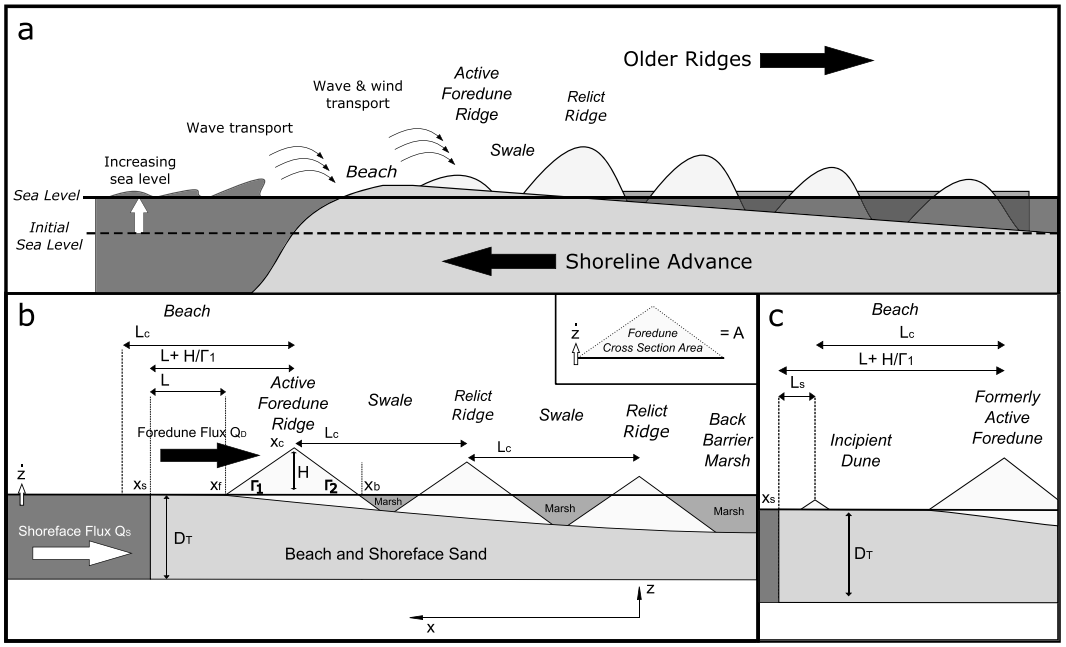

Figure 2. (a) Processes responsible for shoreline progradation. Sand is first transported to the beach (largely through onshore bar migration and contributions from longshore transport) and later transported to the active beach/foredune ridge by aeolian and wave transport. The shoreline advances seaward with time, and new dunes form with a characteristic crest spacing, producing an alternating pattern of ridges and swales. In this example, swales are progressively flooded by rising sea level and experience upland marsh migration from the back-barrier margin. In cases of falling sea level and decreasing shoreface accommodation (also included in model development), this would not occur. (b) Model idealized geometry and processes. (c) Depiction of new dune line emplacement. An incipient foredune forms when the width of the beach and dune flank $L + H/\Gamma_1$ is greater than or equal to the critical ridge spacing plus the setback distance $L_C + L_S$. The crest of the new dune forms at x_s-L_S so that the incipient dune is inland of the shoreline.

example, under constant input, the rate of elevation gain decreases for progressively larger ridges but never results in a steady state, allowing ridges to continue growing until stabilized inland of the active beach.

3. Model Approach and Methods

The observation that nearshore bars form and migrate onshore at rates which scale as a function of sediment input (FitzGerald, 1982) allows us to hypothesize that ridge spacing itself scales proportionally to the flux of sediment to the beach. As such, the spacing of preserved ridges is a proxy for the frequency of bar welding. We therefore parameterize ridge spacing as a measurable component of field morphology which can be used to prompt the formation of an emergent foredune within a model framework. Additionally, as a consequence of the decadal timescales of bar welding, this constrains the applicability of the model to relatively long timescales—the a priori insights at decadal to centennial scales from conceptual models and observations allow us to envision a reduced order system to coarsely control morphology, approximating the ridge formation processes (French et al., 2016) without incorporating specific wind and wave processes responsible for the growth of individual ridges. Notably, even where berm-ridge progradation is not identified specifically as the process responsible for ridge formation, beach sediment fluxes are hypothesized to dominate the morphological response of ridge systems over similar timescales (Oliver, Tamura, et al., 2017), which suggests our first-order parameterization of ridge spacing is sufficient for an initial exploration. Walker et al. (2017) similarly suggests that, at the landscape scale, individual events and processes become less important than the "broader context" of beach-dune interlinkage—the focus of parameterization shifts to the patterns of morphology produced from sequences of events and the sum of background processes.

3.1. Controls on Morphologic Evolution

We propose that the development of foredune ridge and swale system morphology can be broadly controlled by the partitioning of two main components of the sediment budget: fluxes of sand delivered to the beach

and fluxes delivered from the beach to the foredune ridge (Figure 2). In the former, fluxes of sand are delivered to the shoreface and beach through cross-shore and longshore transport. This commonly occurs through the landward migration and welding of nearshore bars, for example, along beaches fed through inlet sediment bypassing (FitzGerald, 1984; Guadiano & Kana, 2001) and strandplain systems in which sediment is sourced from proximal rivers (Nooren et al., 2017; Psuty, 1965). In the latter, sand is transported by tides, waves, and wind from the beach to the foredune by a variety of shallow subaqueous and subaerial physical mechanisms; as such, transport from beach to foredune requires processes that span the foreshore, backshore, and dune line (Cohn et al., 2019). Recent modeling work, field experiments, and observations also suggest that the density of subaerial vegetation (partly controlled by wave climate) strongly modulates the morphology of dunes built primarily by aeolian accretion (Arens et al., 2001; Ruggiero et al., 2018; Vinent & Moore, 2013).

Partly motivating our approach, field observations suggest that shoreface sediment fluxes needed to grow a beach are roughly an order of magnitude larger than sediment fluxes accumulated in foredunes over comparable timescales. A selection of field sites from around the world shows that foredunes generally accrete sediment at a rate of <20 $m^3 \cdot m^{-1} \cdot year^{-1}$ (supporting information Table S1). Comparatively, Himmelstoss et al. (2017) report long-term rates of progradation along the U.S. southeastern Atlantic and Gulf coasts between 8.5 and 33.5 m/year, which, assuming a characteristic shoreface depth of ~5 m, would produce net shoreface fluxes in the range 43–168 $m^3 \cdot m^{-1} \cdot year^{-1}$. The disparity in transport rate between the shoreface and foredune may be as easy to explain as the energy applied to move sand—hydraulic processes are more efficient, with net transport rate decaying rapidly as sand particles move from the subaqueous domain into the intertidal/subaerial domain.

Psuty (2004) observes that rapidly prograding beaches with abundant sediment tend to be composed of many low beach ridges, in contrast to slowly growing beaches with limited sediment availability. Conceptually, slowly prograding beaches develop higher foredune ridges due to greater time to accumulate subaerial sediment. Thus, there is an inverse relationship between ridge size and rate of progradation, which is observed at field sites throughout the world (e.g., Bristow & Pucillo, 2006; Nooren et al., 2017; Oliver et al., 2018). While this relationship has not before been explicitly integrated into numerical models of beach-dune growth, we suggest that envisioning the coast as a two-step partitioning provides a relatively simple means to quantitatively implement this inverse relationship. The dissociation of transport in the subaqueous and intertidal/subaerial domains not only matches well the conceptual progradational model of Psuty (2004) but also allows for more diverse ridge morphology within and between individual coastal systems.

Here, we develop and validate such a numerical model and then apply it, quantifying volume changes in ridge and swale systems through time. Taking a reduced-complexity approach, our model is not intended to directly investigate the physical processes responsible for transporting sediment, focusing instead on the net effect of time-varying sediment fluxes. Our framework is specifically built to produce patterns of subaerial ridge and swale morphology from a simplified sediment partitioning perspective, utilizing idealized ridge geometries. Our field methods and approach thus follow those of Bristow and Pucillo (2006) and Oliver et al. (2015): lidar-derived topography is used to compute subaerial ridge volume, and a combination of sediment coring and ground-penetrating radar is used to measure subsurface volumes. Additionally, as our model results are validated against a study site with a comprehensive historical record, we follow the approach of Kraus and Hayashi (2005) in employing aerial photos to construct a time series analysis of shoreline and ridge-area change.

3.2. Numerical Framework

We use an idealized geometry to model a beach/foredune ridge and swale system (Figure 2), simplifying the process of new ridge formation. As the shoreline progrades, we assume foredunes are formed at a regular spacing for morphologically similar ridges. We apply a critical ridge spacing L_C to define the cross-shore distance threshold at which the beach has grown too far from a given foredune ridge for that ridge to receive sediment, thereby halting its growth and initiating formation of a new ridge. We also assume development of this new foredune does not occur directly on the shoreline, requiring a setback distance L_S per the discussion of Vinent and Moore (2013).

Table 1
State Variables

Symbol	Units	Description
t	T	Time
x_s	L	Shoreline position
x_f	L	Foredune front toe location
x_b	L	Foredune back toe location
x_c	L	Foredune crest location
A	L^3/L	Dune cross-section volume (area)
Z	L/T	Sea level

Based on the idealized geometry depicted in Figure 2b, the evolution of the ridge and swale system is fundamentally described by two state variables: the shoreline location x_s, and the cross-sectional foredune volume A. We describe the change in these boundaries through their modification by shoreface sediment fluxes delivered to the beach Q_S, and fluxes of sand from the beach to the foredune Q_D.

First, the relationship between the aforementioned fluxes and the location of the shoreline is expressed as

$$\frac{dx_s}{dt} = \frac{Q_s}{D_T} - \frac{Q_D}{D_T} - \frac{L\cdot\dot{z}}{D_T} \quad (1)$$

in which $L = x_s - x_f$ is the cross-shore width of the beach, or the distance between the shoreline and the foredune front toe (Figure 2b). Q_S/D_T and Q_D/D_T are the sediment delivery to the beach and the foredune divided by the depth of the shoreface, and $L\cdot\dot{z}/D_T$ is the loss of beach volume to vertical aggradation as a function of sea level rise $\dot{z}$. Although we do not use falling sea level in our field-model comparison, our framework is designed to account for different regional settings, and in this case $L\cdot\dot{z}/D_T$ responds by creating negative accommodation at the beach, extending the shoreline.

Beach-to-dune fluxes grow the cross-sectional volume A of the active foredune ridge, while rising (falling) sea level simultaneously reduces (increases) subaerial volume storage, yielding the following relationship:

$$\frac{dA}{dt} = Q_D - (x_f - x_b)\cdot\dot{z} \quad (2)$$

in which Q_D is sediment input from the beach and $(x_f - x_b)\cdot\dot{z}$ is the loss/gain in subaerial volume due to the effect of sea level change (x_b is the location of the foredune back toe).

We use the cross-sectional volume A of the foredune ridge, modified by sea level rise, and the front and back slopes Γ_1 and Γ_2 to solve for the position of the front and back foredune toes x_f, and x_b using geometric relationships. For our initial model simulations, we assume a triangular foredune profile (although more complex geometries could be used):

$$x_f = x_c + \frac{H}{\Gamma_1} \quad (3)$$

$$x_b = x_c - \frac{H}{\Gamma_2} \quad (4)$$

where x_c is the location of the foredune crest, and the height of the foredune is computed as $H = [2\cdot A/(1/\Gamma_1 + 1/\Gamma_2)]^{1/2}$.

The crest position x_c of a new, incipient foredune ridge relative to the previous ridge crest is given by the critical ridge spacing L_C. When the width of the beach plus the width of the foredune front flank $L + H/\Gamma_1$ is greater than or equal to the critical ridge spacing plus the setback distance $L_C + L_S$ a new foredune will form at x_s-L_S (Figure 2c). Over time, the horizontal position of the foredune ridge crest can be approximated by the following relationship:

$$x_c = (n-1)\cdot L_C \quad (5)$$

where n is the ridge number, increasing in the seaward direction (newer ridges). The position of the first (oldest) ridge is given at $x_c = 0$.

We solve equations (1)–(5) using the Euler method and a time step Δt of 0.1 years over decades to centuries. A full list of the state variables are included in Table 1, while input parameters and descriptions, including a range of explored values, are shown in Table 2. The idealized starting dune and beach geometry is given by initial shoreline and dune crest locations x_s and x_c, dune volume A, and shoreface depth D_T. The beach has a flat slope and maintains elevation with sea level Z. The active foredune is also considered to have constant front and back flank slopes Γ_1 and Γ_2, which define the ridge shape. Additionally, for the purposes of field comparison, we compute total subaerial volume as the profile area of ridges above sea level Z.

Table 2
Model Input Parameters

Symbol	Description/unit type	Fishing Point (Figures 6 and 7)	Parramore Island (Figures 8 and 9)
Q_S	Shoreface flux	134 $m^3 \cdot m^{-1} \cdot year$[a]	1.6 to 15 $m^3 \cdot m^{-1} \cdot year^{-1}$[a]
Q_D	Foredune flux	13 $m^3 \cdot m^{-1} \cdot year$	0.7 $m^3 \cdot m^{-1} \cdot year^{-1}$
L_C	Critical ridge spacing	109 m	117 m
L_S	New foredune shoreline setback	5 m	5 m
Γ_1, Γ_2	Foredune front/back flank slopes	0.05 m/m	0.065 m/m
D_T	Depth of shoreface	5 m	5 m
$\dot{Z}$	Rate of sea level rise	2 mm/year	1 mm/year

[a]Fishing Point sediment fluxes are derived from time series analysis of shoreline and subaerial elevation change; Parramore Island fluxes are derived from morphological calibration. See sections 4.1 and 5.1 for additional input parameter discussion.

3.3. Exploration of Model Behaviors

Based on the theoretical framework of Psuty (2004) and a variety of field observations (Bristow & Pucillo, 2006; Nooren et al., 2017), we conceptualize the end-members of ridge and swale systems under different sediment input regimes. The fastest rates of progradation—relatively high beach flux and low foredune flux—should lead to numerous, low-elevation ridges or open sand flats. Conversely, the slowest rates of progradation—low beach flux and high foredune flux—should result in the formation of fewer, prominent ridges or a monolithic foredune. Additionally, observations of coastal systems such as Fishing Point (Figure 1) indicate that regularly repeating ridges of moderate elevation or "washboards" should occur between the aforementioned endmembers. Thus, in order to classify ridges in the field, and using our modeling framework, morphological members are categorized according to Figure 3.

In order to explore endmember ridge morphologies in the context of input fluxes, we consider differences in the magnitude of Q_S versus Q_D from natural systems. Based on the work of Himmelstoss et al. (2017), we consider Q_S values within the range 0–200 $m^3 \cdot m^{-1} \cdot year^{-1}$. Additionally, we consider Q_D values within the range 0–20 $m^3 \cdot m^{-1} \cdot year^{-1}$, as determined from a global compilation of foredune accretion rates (Table S1). We note that it is possible to run the model with negative Q_S values (i.e., net erosion) for brief intervals of time—all of the existing equations could be run backward. However, sustained shoreline retreat would require additional conditions to erode and/or trangress the active foredune (e.g., through scarping or otherwise reducing the idealized foredune profile, as well as possibly returning eroded volume to the shoreface).

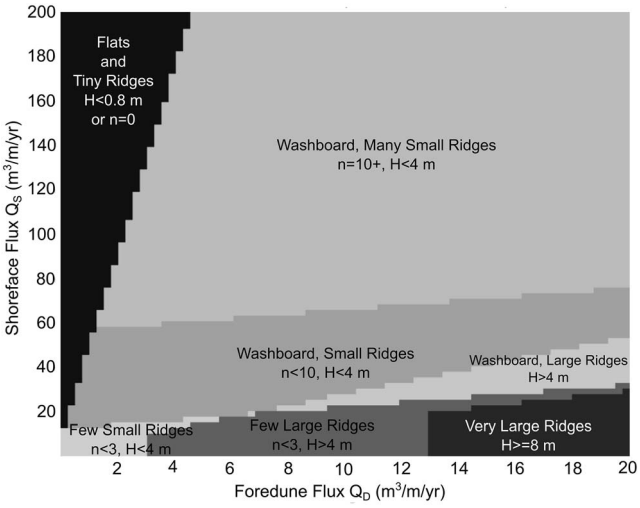

Figure 3. Regime plot showing the types of subaerial ridge and swale patterns modeled over the timescale of Fishing Point (100 years) for combinations of shoreface fluxes Q_S and foredune fluxes Q_D. Our characterization of ridge heights is based on the tallest ridges observed in the Virginia system (8 m). The rate of rise was set to 2 mm/year, and the critical ridge spacing was 109 m. To distinguish patterns, n = number of ridges and H = height of ridge.

Within the modeled input space, we find that we can broadly create washboards when Q_S is approximately an order of magnitude larger than Q_D (Figure 4a). Modulating this sediment input regime by increasing Q_S by another order of magnitude yields sand flats and tiny ridges (Figure 4b). Such morphologies are readily observable in the field: central Parramore Island contains a large swale-like structure approximately 0.7 km wide (Raff et al., 2018), and in Sandy Hook (New Jersey, USA), both wide, interridge swales and sand flats that extend up to 400 m in width are present (National Park Service, 2016). Conversely, reducing Q_S to within the same order of magnitude as Q_D yields relatively large ridges (Figure 4c); this morphology mimics that of the 7+ m high Italian Ridge located on northern Parramore Island (Figures 1c and 1e).

3.4. Field Comparison

We model the sediment budget history of a set of beach and foredune ridges as a series of morphological patterns with distinct flux regimes, generating ridge sets with characteristics that can be compared with measurements of field sites. Specifically, measurements readily captured by our

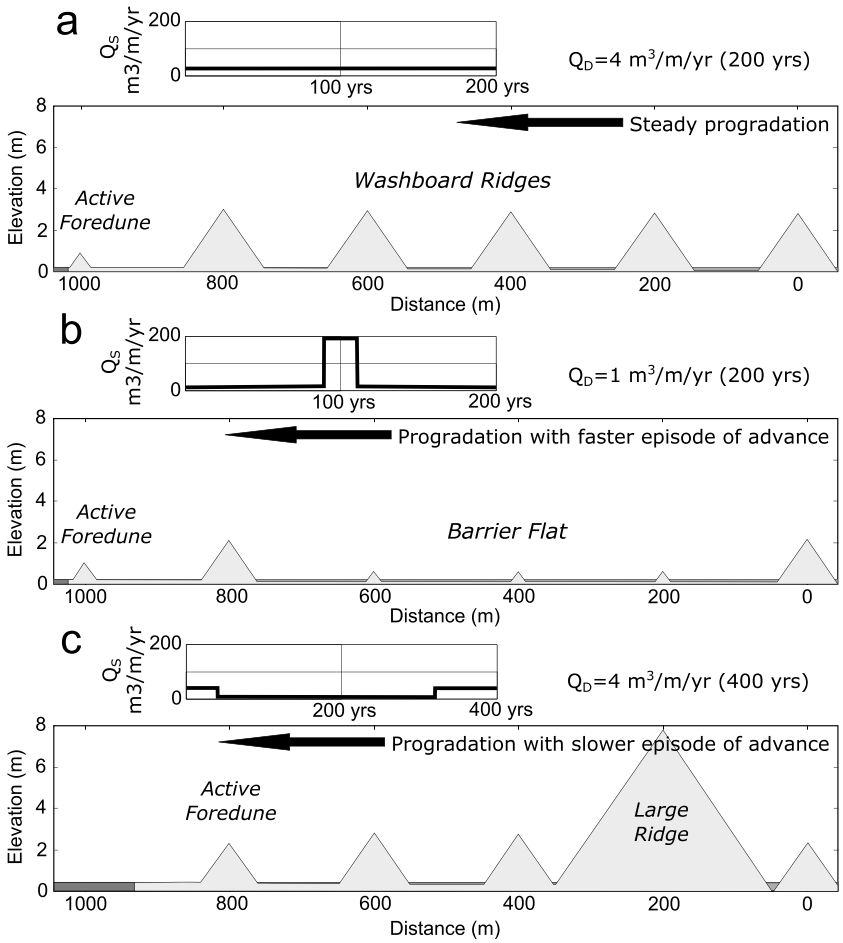

Figure 4. Modeled pattern of cross-shore changes in ridge geometry resulting from adjustments in the rate of progradation by modulating Q_S. (a) Washboard pattern of regularly spaced ridges, with steady Q_S. (b) Episode of fast progradation that suppresses ridge height and results in a wide flat on the barrier platform. (c) Sustained episode of slow progradation, allowing time to build a large ridge. For all cases, $L_C = 200$ m, $L_S = 5$ m, with rate of rise of 1 mm/year.

modeling framework include the subaerial volume of ridges, the number of ridges formed during progradation of the shoreline by a given distance (a function of ridge spacing), and the height of ridges. These are characteristics readily measurable using lidar data and other geophysical approaches. In this study, we measure elevation profiles perpendicular to the ridge system at our two Virginia field sites using the 2016 Coastal National Elevation Database lidar digital elevation model (Figures S1 and S2). Ridges in these systems do not have uniform crests as a result of erosion/reworking by waves, wind, and vegetation, and/or incomplete initial amalgamation (Raff et al., 2018). As such, they commonly display mottled surfaces consistent with either vegetation-induced nebkha (coppice dunes), wave-induced washarounds, or mounds formed through a combination of processes. To account for this alongshore variation, ridge crests are manually delineated in plan view using high-resolution elevation maps (Figure S15)—we note that in systems with more regular ridges or better ridge preservation (e.g., strandplains), more rigorous methods of supervised/unsupervised ridge delineation using slope and elevation change could be employed. Furthermore, to make a comparison with our two-dimensional model, we average elevation profiles every 10 to 20 m across a 100-m-wide (alongshore) swath to produce a profile that reflects a mean cross-shore ridge structure along our study transects (Figures 1d and 1e). We measure the critical ridge spacing L_C by taking the average crest-to-crest spacing from the mean profile.

To correlate lidar-derived elevations and subaerial ridge volumes with model outcomes, we use the lowest elevation of swales as a common point of reference. Lidar measurements along the Virginia barrier islands indicate that the base of swales, and in particular of those now flooded by rising sea level, are at an elevation

of approximately mean higher high water (MHHW) for both Parramore Island and Fishing Point (Table S2). This elevation corresponds to the tidal inundation boundary that the National Oceanic and Atmospheric Administration uses to map the marsh-upland transition (NOAA, 2017) and has been used in geographic studies to approximate the limit of upland marsh migration (Archbald, 2010).

Finally, in determining the setback distance of incipient foredune ridges for our model simulations, we note in Vinent and Moore (2013) that foredune height scales in proportion to setback; ridges become capable of growing (initially) larger as the beach area grows in conjunction with increasing aeolian sand fetch. For our investigation, we try $L_S = 5$ m, as Vinent and Moore (2013) show that a setback of 10 m for a reasonable range of shear stress values produces a ridge approximately 1–2 m in height—double the height of the lowest ridges observed at our field sites. The current framework also assumes L_S remains constant through time and so does not account for changes in beach slope or vegetation density between or during ridge formation episodes, which could affect incipient foredune shape and placement (Hesp, 2011).

4. Model Validation: Analysis of the Growth of Fishing Point, Virginia

To validate our model framework, we use the historical record available from Fishing Point to conduct a time series analysis of Q_S and Q_D and supply these directly to the model. This allows us to compare the morphological characteristics of modeled cross sections directly to field observations. A subsequent sensitivity analysis of morphological characteristics based on mean fluxes through time for Fishing Point demonstrates that we can determine an average long-term sediment budget based on measurements of field characteristics alone. In section 5, we use this insight to derive Q_S and Q_D for morphological patterns of ridges at Parramore Island, where construction of a time series of ridge development is not possible from existing data.

4.1. Fishing Point Overview

Fishing Point (Figures 1b and 1d) is a southward prograding spit constructed at the southernmost point of Assateague Island. It receives sediment through southerly longshore transport at a rate of 0.16–1.1 $\times$ 10^6 m^3/year (Finkelstein, 1983; Headland et al., 1987; Moffatt and Nichol, Engineers, 1986). Coast and Geodetic survey charts (Figures S3 and S4) indicate that its subaerial growth initiated sometime after the mid-1850s, although formation of the recurved spit end, and associated coast-perpendicular ridge development, did not begin until the early twentieth century. Between 1908 and the present, Fishing Point prograded nearly 2.5 km through the amalgamation of at least 20 distinguishable foredune ridges (Table S3 and Figure S5). The upper surface of ridges tends to be irregular, likely as a result of incomplete amalgamation or modification by waves and vegetation.

Survey charts show former seabed depths in the area of Fishing Point were generally around 5 m, providing an estimate of the modern shoreface thickness. Likewise, a sediment core approximately located at the 1902 shoreline of the spit (Halsey, 1978) indicates that barrier sands are ~5 m thick. Based on lidar and aerial images (Figures 1 and S5), the overall ridge morphology is relatively regular, with ridges averaging 1 m in height and with an average crest spacing L_C of 109 m. Generally, ridges are symmetric, with front and back slopes near 0.05 m/m (Figure S6). Total subaerial cross-sectional volume through the longest ridge-perpendicular transect is 1,300 m^3/m.

Fishing Point experienced a mean, long-term rate of progradation (southerly elongation) of ~24 m/year, with a corresponding beach sediment flux of ~120 $m^3 \cdot m^{-1} \cdot year^{-1}$ (Figure S7). However, the maximum progradation rate estimated from Landsat imagery and nautical charts over the last 35 years is 41.8 m/year and possibly higher in recent years. This increase in progradation may be related to a shift in sediment depocenter along the Fishing Point shoreline (Hein et al., 2019) and/or beach nourishment on the northern end of Assateague Island, ongoing biannually since 2002 and supplemented by berm reconstruction approximately every 4 years (Smith et al., 2016). Nourishment volume lost to longshore transport updrift of Fishing Point totals almost 380,000 m^3/year (Smith et al., 2016). If that updrift volume is completely distributed over the actively prograding face of the southern-most part of the spit (~1.5 km alongshore), the theoretical modern progradation rate is 51 m/year, not considering additional inputs (e.g., cross-shore fluxes from the shallow shelf). Presumably, some portion of this missing volume is also bypassed across Chincoteague Inlet to islands further downdrift.

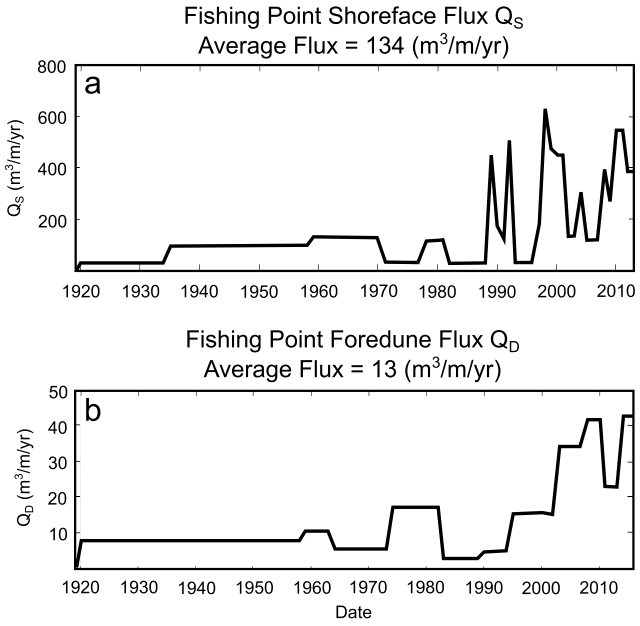

Figure 5. (a) Calculated shoreline fluxes for the Fishing Point transect for 1919–2013. The average flux for this period is 134 $m^3 \cdot m^{-1} \cdot year^{-1}$. (b) Calculated foredune fluxes for the Fishing Point transect for 1958–2016. The average flux for this period is 13 $m^3 \cdot m^{-1} \cdot year^{-1}$.

4.2. Deriving Input Fluxes From the Historical Record

In model simulations, sediment fluxes to the beach Q_S and the foredune Q_D during the historical period of growth of Fishing Point are given as time-varying input parameters which are derived from historical imagery. We attempt to compute Q_S using a 95-year (1919–2014) record of digitized former shorelines. By overlaying shoreline locations on the cross-ridge elevation profile (Figure S11), it is possible to divide the profile into intervals of sediment delivery and calculate a time-averaged shoreface flux (Figure 5a).

Determining foredune fluxes Q_D requires a means by which to separate foredune ridge sand from beach sand. If we assume minimal impact from sea level rise, the simplest solution is to use MHHW as a threshold elevation between the two units. However, foredune emplacement, driven by a complex interplay of wave and aeolian transport, lags the advance of the shoreline. As a result, changes in subaerial volume cannot be calculated directly from sediment delivery to the beach.

To compute foredune fluxes through time, we develop a timeline of foredune emplacement independent of changes in shoreline position. We use historic aerial photos to determine the first known date individual ridges or sets of ridges became relict; that is, when they are no longer adjacent to the beach or substantially accreting. High-resolution aerial photos extending back to 1958 provide nearly six decades of observations on which to develop a progression of ridge abandonment (Figure S5) and a corresponding quantification of subaerial volumetric growth based on the transect elevation profile (Figure S12). Foredune fluxes are then calculated over a 58-year period ending in 2016 (Figure 5b).

4.3. Modeled Fluxes and Morphology

The growth of Fishing Point was evaluated in the model framework using a time series of input fluxes derived from the historical record and compared to field observations using average ridge height, ridge cross-sectional volume, and number of ridges within the distance prograded by the shoreline (Tables 3 and S3). Over 95 years, the model produced washboard-like morphology with characteristics measured to within the same order of magnitude as field estimates (Figure 6b). The greatest discrepancy between modeled morphology and field measurements occurs for dune height: the model produces ridges approximately 50% taller than those measured from lidar (Table 3).

Table 3
Modeled Versus Field Measurements

Parameter	Field	Model	Difference Field − Model	% Diff. to Field
Fishing Point time series				
Total cross-section volume (m^3/m)	1,295	1,073	222	−16.2%
Average ridge height (m^3/m)	1	1.5	−0.5	+50%
Distance prograded (m)	2,290	2,181	109	−5%
Number of ridges	20	20	0	0%
Fishing Point average fluxes				
Total cross-section volume (m^3/m)	1,295	1,214	82	−6%
Average ridge height (m^3/m)	1	1.6	0.6	+60%
Distance prograded (m)	2,290	2,237	53	−9%
Number of ridges	20	21	−1	+5%
North Parramore "Back Four" (200 years)				
Total cross-section volume (m^3/m)	140	133	7	−5%
Average ridge height (m^3/m)	0.6	1.3	−0.7	+110%
Distance prograded (m)	500	483	17	−3%
Number of ridges	4	4	0	0%

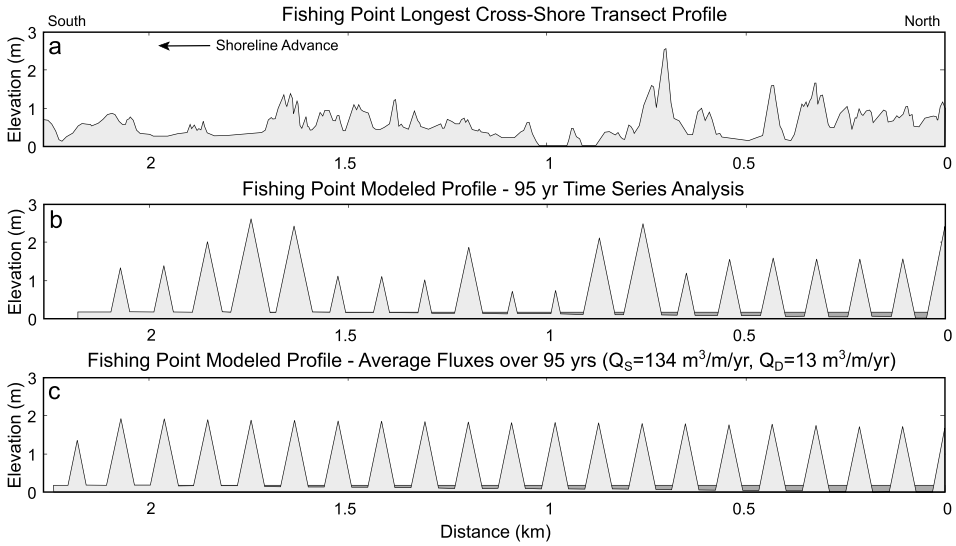

Figure 6. (a) Elevation cross section of Fishing Point along its widest dimension measured from lidar data. (b) Modeled profile of Fishing Point using a time series of shoreface and foredune fluxes derived from the historical record. While the average height of the modeled profile is 50% taller than the field average, the remaining parameters are within 20% of field measurements (Table 3). (c) Modeled geomorphological profile of Fishing Point using a time-invariant shoreface flux Q_S of 134 $m^3 \cdot m^{-1} \cdot year^{-1}$ and a foredune flux Q_D of 13 $m^3 \cdot m^{-1} \cdot year^{-1}$, the long-term average flux values derived from the historical record.

We also ran a sensitivity analysis of the input flux space (Figure 7), allowing us to constrain a range of average fluxes that produce a more generalized washboard pattern (Figure 6c). Actual measurements of morphologic characteristics are highlighted as key contours and are used to construct a morphological calibration plot (Figure 7e), which identifies a region of similarity where flux combinations generally reproduce measurements from the field. For Fishing Point, average historical Q_S and Q_D values occur within this region of fluxes, near the contour for subaerial ridge volume. Comparison of modeled average height and spacing values (Figure 6c) to remote observations (Table 3) produces results similar to our time series model-field comparisons, including the discrepancy in ridge height. While the model does not fully capture real-world ridge heights, it reasonably reproduces the overall sediment balance, as well as the partitioning between subaerial and subsurface volumes.

5. Model Application: Reconstructing the Growth of Parramore Island, Virginia

Field-based model validation demonstrates that use of characteristics of beach and foredune-ridge morphology may allow for the reconstruction of long-term shoreface sediment budgets and, notably, the magnitude of time-varying sediment fluxes. To evaluate the capabilities of the model, it is next applied to an investigation of Parramore Island. We use a limited chronology based on OSL and radiocarbon dating to constrain the development of the complex beach and foredune ridge system on the northern half of the island. Then, using morphological characteristics observed in the field, we use the model to calibrate the range of input Q_S and Q_D values for sections of the ridge and swale complex and apply this to simulate development of a cross-island, two-dimensional morphological profile for field comparison.

5.1. Parramore Island Overview

Parramore Island (Figure 1c and 1e) is 11 km long and located ~36 km south of Fishing Point. It is a historically rotational (undergoing erosion of its southern end and progradation at its northern end), mixed-energy barrier island that, prior to the early twentieth century, maintained a drumstick-like shape (Deaton et al., 2017; McBride et al., 2015). Humans have never occupied the island continuously, and it has existed in a near-natural state since it was first documented (Rice et al., 1976).

Northern Parramore Island contains two sets of northeast to southwest striking, low-relief washboard ridges (the “Back Four” and “Front Four” ridges) that flank a large, central ridge (Italian Ridge). Whereas the average elevation of northern Parramore is ~1.1 m (MHHW), the maximum elevation along Italian Ridge is >7 m

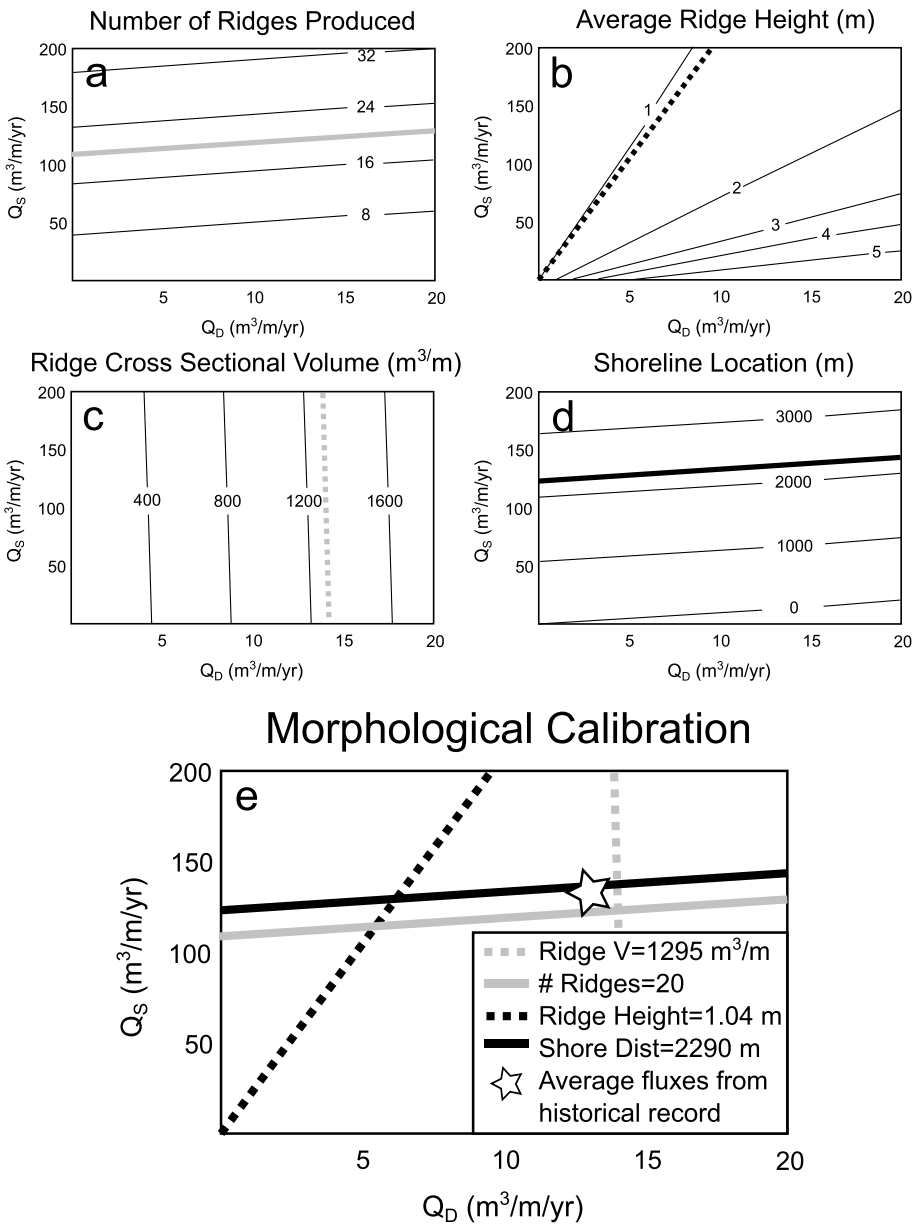

Figure 7. Sensitivity plots of (a) number of ridges produced, (b) average ridge height, (c) cross-sectional dune volume, and (d) final shoreline location, as a function of input-flux combinations. Bolded contours represent measurements of the four morphologic parameters obtained from the field at Fishing Point. (e) A morphological calibration in which the area bound by the intersection of the four parameter lines—the *region of similarity*—indicates the range of flux combinations that produce results similar to field measurements.

(Figure 1 and Table S4). Remaining ridges reach generally no more than 60 cm in elevation. Despite hummocky topography, the low washboard ridges have an average profile that is triangular and slightly asymmetric. The westernmost "Western Ridge" is the best preserved, with a front slope of 0.012 m/m and a back slope of 0.018 m/m (Figure S8). The slopes of Italian Ridge are an order of magnitude steeper, at 0.125 m/m and 0.11 m/m (Figure S9). In our modeling exercise, we set a mean slope for Parramore Island of 0.065 m/m, which attempts to account for the difference in slope between Italian Ridge and its smaller counterparts (Figure S13 depicts a sensitivity analysis of ridge height as a function of slope and shoreface accommodation). Regressive barrier island sands beneath the ridges extend to 4.5–5.0 m below MHHW, and the underlying transgressive surface is nearly horizontal from the modern foredune to west of Italian Ridge, located about 600 m landward (Raff et al., 2018).

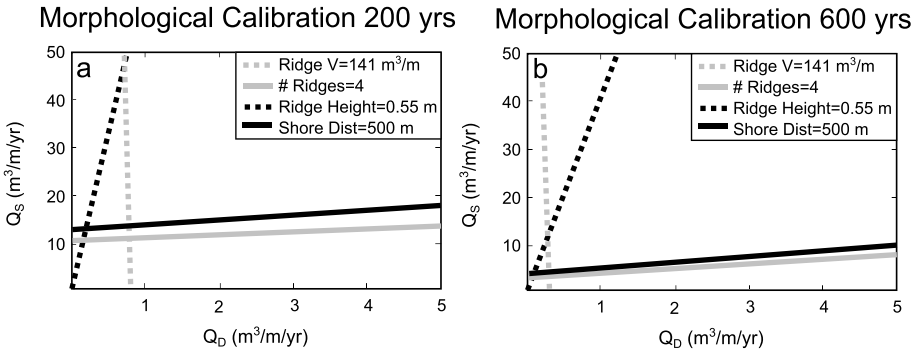

Figure 8. Evaluation of the "Back Four" ridges of North Parramore Island using morphological calibration plots to constrain the balance of Q_S and Q_D fluxes consistent with field sites parameters over timescales of (a) 200 years and (b) 600 years. The area bound by the intersection of the four parameter lines—the *region of similarity*—indicates the range of flux combinations that produce results similar to the field.

Though once transgressive, landward migration of Parramore Island ended ~1,000 years ago and has been followed by a period of slow progradation lasting at the northern end of the island until the mid-1950s (Raff et al., 2018). Italian Ridge was dated with OSL to about 200 years ago (this likely represents the time at which this former foredune became inactive; Raff et al., 2018), and historical maps indicate that the northern Parramore shoreline reached its maximum seaward position by the late 1800s (Rice et al., 1976).

5.2. Modeled Fluxes and Morphology

Parramore Island presents an opportunity to apply our model to a site with a poorly constrained prehistoric record of growth to explore Q_S and Q_D flux combinations that reproduce patterns of observed ridge morphology. Due to the location of age control points, we first consider the growth of the Back Four washboard ridges and of Italian Ridge, which together developed over a period of ~800 years from the inception of Western Ridge (1000 CE) to the abandonment of Italian Ridge (1800 CE). The initiation of growth for Italian Ridge, a time stamp which would constrain the period of formation of the Back Four, is unknown, but an informed guess is possible. The western four ridges are morphologically similar to the eastern (seaward) four ridges, which developed over a period spanning at least the mid-1700s to the early twentieth century (Rice et al., 1976). This morphological resemblance suggests a similarity in formation processes and time; from this we estimate a period of growth of ~200 years for the development of the Back Four ridges. We apply an upper limit of 600 years as a maximum period of growth.

Assuming a 200-year period of development, the Back Four washboard was evaluated in the model framework using field-derived morphological characteristics (Table 3). From morphological calibration plots (Figure 8), we selected a Q_S and Q_D flux combination (Q_S = 13 $m^3 \cdot m^{-1} \cdot year^{-1}$ and Q_D = 0.7 $m^3 \cdot m^{-1} \cdot year^{-1}$) that adequately reproduced subaerial volume, distance prograded, and number of ridges produced. The morphological characteristics of the washboard ridge system resulting from this flux combination are within 5% of bounds from field measurements, except for average ridge height (Table 3).

Calibration plots (Figure 8) show the range of shoreface flux Q_S and foredune flux Q_D combinations that produce results consistent with the morphology of the western and eastern washboard ridge sets on Parramore Island are an order of magnitude smaller than those determined for Fishing Point. This result implies the shoreface flux must be even smaller to create the 7-m-tall Italian Ridge. Using a constant Q_D of 0.7 $m^3 \cdot m^{-1} \cdot year^{-1}$, and conserving all other input parameters, we attempted to reconstruct the full profile of north Parramore Island, allotting 200 years to build the Back Four washboard ridges, 600 years to build Italian Ridge, and another 200 years to build the Front Four washboard ridges. The model best reproduced the morphology of Italian Ridge when Q_S was reduced by an order of magnitude, to 1.6 $m^3 \cdot m^{-1} \cdot year^{-1}$. The Front Four ridges were then approximated with Q_S values returned to 15 $m^3 \cdot m^{-1} \cdot year^{-1}$ (Figure 9).

Historically, the average progradation rate of north Parramore Island was 1.9 m/year from 1852 to 1955 (Rice et al., 1976); this closely matches the progradation rate (2.4 m/year) given by our model (Figure 9b). However, our investigation does not account for the increased rate of sea level rise since the late 1800s: tide gauges in the vicinity of the Delmarva Peninsula indicate the current rate of rise is between 3 and 5 mm/year (Boon &

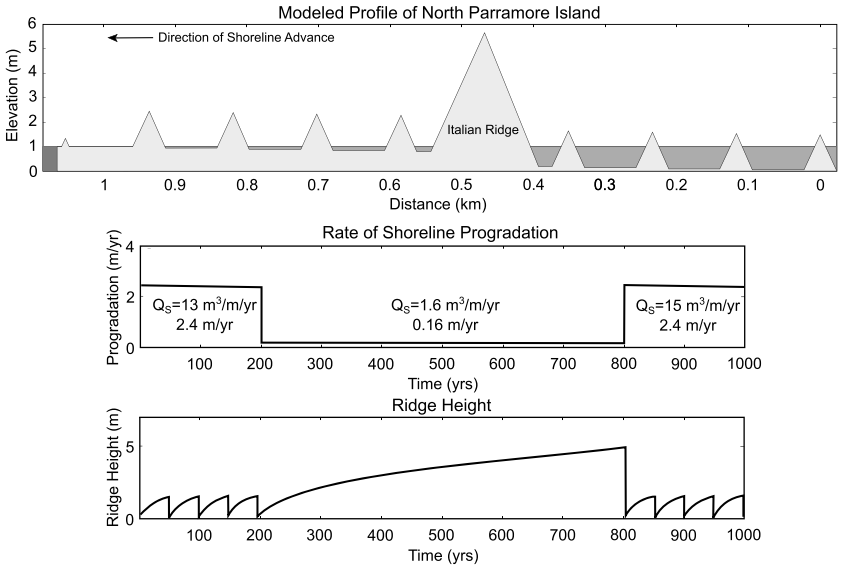

Figure 9. (a) Modeled geomorphological profile of North Parramore Island using a shoreline flux Q_S of 13 $m^3 \cdot m^{-1} \cdot year^{-1}$ for 200 years, 1.6 $m^3 \cdot m^{-1} \cdot year^{-1}$ for 600 years, and 15 $m^3 \cdot m^{-1} \cdot year^{-1}$ for the last 200 years—with a constant foredune flux Q_D of 0.7 $m^3 \cdot m^{-1} \cdot year^{-1}$. Changes in (b) rate of shoreline progradation and (c) ridge height are shown for the 1,000-year run time of the model.

Mitchell, 2015). Instead, our model applies the long-term preindustrial estimate of 1.0 mm/year (Engelhart & Horton, 2012) as a constant rate throughout the period of development of Parramore Island. This difference may partially account for the faster (by 0.5 m/year) rate of progradation reproduced by our model, as overall vertical accommodation available in the modeled ridge system is ~30–50 m^3/m less than that created by sea level rise in the real-world system (see Figure S14 for additional sea level sensitivity analysis).

One component not captured by our model is the development of the modern transgressive foredune (~1.6 m elevation), which on northern Parramore has formed over the last ~70 years. While our model does not capture transgression, Psuty (2004) shows that trangressive foredunes probably occur only for beaches undergoing relatively slow erosion: the landward transport of sediment has to outpace losses on the seaward edge; otherwise the foredune quickly erodes. As a consequence, transgressive foredunes should (hypothetically) not exist under input conditions which differ significantly from those which occur under static or slow shoreline progradation. Coincidentally, the height of the transgressive foredune in the modern Parramore system roughly agrees with model predictions for 70 years of ridge growth.

For Italian Ridge, it is possible that long-term progradation was interrupted by one or more periods of beach erosion and foredune transgression, but sediment input at the beach during such a period may well have been within the same order of magnitude as our modeled value. The plan view morphology (Figure 1c) also suggests such erosion probably did not occur over long timescales, because the orientation of the ridge axis is effectively parallel with the ridges landward of Italian Ridge, a feature not shared with the subparallel modern transgressive foredune. Changes in the orientation of transgressive foredunes (relative to relict ridges) are common along other beach-ridge plains (Oliver, Donaldson, et al., 2017; Psuty, 2004), including on nearby Assateague Island. Only the northern and southern ends of Italian Ridge are shifted out of alignment with adjacent ridges, likely as a result of erosion associated with inlet activity (Raff et al., 2018).

6. Discussion

6.1. Parramore Island

The planar, near-horizontal transgressive surface upon which Parramore Island prograded makes it an ideal site to record externally mediated changes in shoreface sediment fluxes, as accommodation effects such as growth into an offshore-deepening basin (e.g., Bristow & Pucillo, 2006) or into an infilling bay (e.g., Hein et al., 2016) are minimal. Hence, the rate of progradation of this barrier island should reflect only the rate of sea level rise and net (longshore and cross-shore inputs minus long-term erosion) external sediment

fluxes. Assuming long-term (multi-decadal through centennial) shoreface sediment fluxes are primarily derived from sediment delivered through the southerly longshore transport system, then changes in the progradation rate of northern Parramore Island—and by extension, changes in the morphology of associated foredune ridges—reflect changes in the rate of allogenic sediment delivery. Along the Virginia barrier islands, longshore sediment fluxes are controlled by such factors as updrift inlet configurations and sediment-bypassing processes (FitzGerald, 1984), sediment trapping in flood-tidal deltas associated with ephemeral inlets (Seminack & McBride, 2015), variations in ebb-tidal delta storage (Fenster et al., 2016), and disruptions in sediment supply associated with the growth and erosion of updrift spits and islands (McBride et al., 2015; Raff et al., 2018). For example, Fishing Point itself—located updrift of the mixed-energy barrier islands to the south—traps sand at a rate of up to 1.1×10^6 m^3/year (Moffatt and Nichol, Engineers, 1986), removing it from the longshore transport system. Without this substantial sediment sink, an additional ~11.6 $m^3 \cdot m^{-1} \cdot year^{-1}$ of sand could be distributed to the shoreface of all islands to the south (~95 km of beach). This flux is significant: our investigation shows that the net growth of Parramore Island has been slow, on the order of a few meters per year over the last thousand years, and operating on a net cross-shore sediment budget of 15 $m^3 \cdot m^{-1} \cdot year^{-1}$ or less. In the context of the Virginia system, where overwash-driven landward migration and erosion dominates the response of barriers under low shoreface sediment flux conditions, we suggest Parramore Island's marginal rate of progradation (barely maintaining long-term seaward advance) renders it particularly vulnerable to changes in sediment fluxes consistent with the magnitude of trapping at Fishing Point. Our results support the hypothesis proposed by Raff et al. (2018) that the Virginia barriers are subject to rapid state transitions (between net erosion, progradation, and migration) resulting from downdrift-cascading sediment supply deficits.

6.2. Broader Application

Globally, beach- and foredune-ridge systems are diverse and complex. Some have morphologies similar to Fishing Point, characterized primarily by repeating sets of low-elevation ridges (e.g., Samso, North Sea, Hede et al., 2013; Pinheira, Brazil, Hein et al., 2013), or are more characteristic of Parramore Island, dominated by low-elevation ridges with rare, much higher individual ridges (e.g., Miquelon-Langlade, France, Billy et al., 2014; Seven Mile Beach, Australia, Oliver, Donaldson, et al., 2017). Application of our model to each of these progradational systems could allow for quantification of sediment-flux conditions associated with their development, potentially providing insights on sensitivity to future environmental change.

In particular, our findings may be most applicable to strandplains, broad accumulations of sediment formed as beach and foredune ridges oriented approximately parallel to the coastline (Roy et al., 1994). These are typically characterized by long-term, continuous progradation of successive ridges and swales. As compared with beach- and foredune-ridge systems on barrier islands, strandplain ridge systems are less likely to be punctuated by inlet activity and are particularly common in regions of stable or falling sea level (Tamura, 2012). Variability in progradation rates observed across strandplain systems has been attributed to differences in coastal slope, sediment supply, accommodation, wave energy, and sea level history (Choi et al., 2014); our model could provide quantitative insight into the role of each of these. For instance, the punctuated growth of strandplain systems like Seven Mile Beach, Australia, has been linked with variations in shoreface fluxes driven by possible changes in the rate of sea level rise (Oliver, Donaldson, et al., 2017). A similar deceleration in shoreline growth at Pedro Beach, Australia, may be linked to changes in accommodation (Oliver et al., 2018). A possible concern is that the rates of strandplain progradation (0.4–1.8 m/year; Bristow & Pucillo, 2006; Brooke et al., 2008; Hein et al., 2016) are generally lower than those observed in our barrier island study sites. However, as we demonstrate through application of our model to Parramore Island, the model can be used at sites undergoing slower progradation (i.e., 0.16 m/year; $Q_S = 1.6$ m/year), particularly if corresponding foredune fluxes are also low (i.e., $Q_D = 0.7$ m/year). Furthermore, strandplains can experience episodes of progradation similar to those we demonstrate in the initial test of our model (e.g., ~7.8 m/year; Bristow & Pucillo, 2006).

6.3. Considerations and Future Work

Our model partitions subaerial sediment volume into idealized ridge geometries and so does not yet capture impacts associated with vegetation or erosional reworking. As such, field calibration requires an assumption of a high degree of preservation of ridge morphologies. For example, segmentation of foredune ridges by former inlets further south along Parramore Island (Raff et al., 2018) renders that portion of the island ridge

system unsuitable for model application. However, we show that through averaging of elevations of ridge transects across an alongshore swath, we can adequately reconstruct topographic profiles of even moderately degraded ridges. Specifically, our investigation suggests the number of topographic profiles used to develop an alongshore-average profile should scale with ridge slopes: broad, gently sloping ridges (northern Parramore) require fewer profiles to integrate than steeper, more discrete ridges (Fishing Point).

Among the field parameters used to perform morphological calibrations, our implementation of ridge height could be further refined. For example, we use an average, site-wide ridge slope for Fishing Point and Parramore Island to inform model geometry, and our results generally overestimate height. Examining a sensitivity analysis of modeled ridge heights to slope (Figure S13), we find that, in the example of the Parramore Island Back Four ridges, our use of an island-averaged slope (0.065 m/m) could produce ridges slightly more than 0.5 m taller than would be produced by more exact slope measurements of those specific ridges. While this is a small deviation, it is within the same magnitude as the actual ridge heights, which suggests our triangular idealization of ridge geometry is less a source of discrepancy than our choice of slope. However, for sustained washboard patterns with a larger number of ridges (e.g., Fishing Point), this outcome could present challenges if ridge slope varies considerably from ridge to ridge. One possibility is that, because the foredune ridges along Fishing Point are more spatially discrete than those on Parramore, deviations in ridge slope occur more readily from wind/wave reworking during and following ridge formation.

Finally, our model can be reconfigured in a variety of ways to account for other subaerial and subaqueous processes/geologic controls. For the field sites evaluated in this study, we employed a constant seabed elevation and rate of sea level rise, but the model is already built to investigate changes in accommodation through, for example, nonuniform offshore slopes (growth into deep basins or shallowing bays) or alterations in the rate and/or direction of sea level change (Figure S14). It can thus be readily applied to the many well-studied beach- and foredune-ridge plains formed in regimes of sea level fall (e.g., Bristow & Pucillo, 2006; Hein et al., 2013, 2016; Oliver, Donaldson, et al., 2017). Application to long-lived strandplain systems, which often feature complex patterns of ridges, may additionally allow for variable ridge spacing with time, offering a field-comparative means to explore ridge formation versus long-term progradation rate. Beyond simple reconfigurations, future extensions could also include grain size partitioning, stochastic storm/episodic erosion, and conversion of prograded ridges to transgressional dunes—potentially important considerations discussed by Billy et al. (2014) and Oliver et al. (2017), among others.

7. Conclusions

We demonstrate a simple framework to quantify the magnitude of changes in cross-shore sediment budget for prograding beach- and foredune-ridge systems by making use of the morphology of subaerial ridge and swale complexes. Within our model, the development of ridge and swale morphology is constrained by fluxes of sediment to both the foredune ridge system and the shoreface. Partitioning of these fluxes gives rise to cross-shore morphologies we define as flats, washboards, and large ridges. We use our framework to perform a morphological calibration on these patterns at field sites along the northern Virginia Atlantic coast, employing field and remote measurements of subaerial ridge volume, spacing (number of ridges), ridge height, shoreline progradation distance, and geochronology to derive time-varying net sediment budgets.

Our results offer insight into the development of the Virginia barrier islands, suggesting that a marginal sediment budget could influence historical state shifts of islands between relative stability/progradation and rapid erosion. Moreover, we suggest our model could provide an intuitive means to explore the sediment supply history of strandplains and prograding barrier systems around the world, especially with future model extension. We envision this model will add perspective in existing investigations where geochronological control is limited, as well as enable insights into accommodation effects, notably those arising from changes in the rate of sea level rise and presence of variable offshore bathymetry. Application of the model to further field sites (e.g., strandplains with complex patterns of well-preserved ridges) will also enable rigorous sensitivity analyses and field comparisons for input parameters, especially inputs which capture ridge geometry.

Acknowledgments

This research was supported by both the New Jersey Sea Grant Consortium (NJSGC) and Virginia Sea Grant (VASG), through the Mid-Atlantic Regional Sea Grant Program. All funds come from the National Oceanic and Atmospheric Administration (NOAA) Office of Sea Grant, U.S. Department of Commerce, under NOAA grant number NA14OAR4170085 (NJSGC) and grant numbers R/71856G and R/71856H (VASG). The statements, findings, conclusions, and recommendations are those of the author(s) and do not necessarily reflect the views of the NJSGC, VASG, or the U.S. Department of Commerce (NJSG-18-937). Additionally, D. J. C. and C. T. received support from the Department of Earth and Environmental Studies at Montclair State University, and J. L. S. from the Virginia Institute of Marine Science/School of Marine Science Office of Academic Studies. This manuscript benefitted immensely from thoughtful evaluations by S. de Vries and two anonymous reviewers, as well as guidance from JGR Editors, C. Storlazzi and G. Coco. We also thank A. Janoff, J. Kolodin, I. Cortés, and W. Anderson for their feedback during model development and application. Supporting information, analyses, and data are provided in the accompanying supporting information. A copy of the model script (MATLAB) used in this study, as well as scripts and data to examine and produce time series from our elevation profiles, are available at our model development page (https://github.com/ciarletd/Beach-and-Foredune-Ridge) and archived under DOI: 10.5281/zenodo.2575699. This paper is contribution 3828 of the Virginia Institute of Marine Science, William & Mary.

References

Aagaard, T., Davidson-Arnott, R., Greenwood, B., & Nielsen, J. (2004). Sediment supply from shoreface to dunes: Linking sediment transport measurements and long-term morphological evolution. *Geomorphology*, *60*(1-2), 205–224. https://doi.org/10.1016/j.geomorph.2003.08.002

Archbald, G. (2010). Merging tidal datums and lidar elevation for species distribution modeling in South San Francisco Bay. Report prepared for the South Bay Salt Pond Restoration Project, Alviso, CA.

Arens, S. M., Baas, A. C. W., Van Boxel, J. H., & Kalkman, C. (2001). Influence of reed stem density on foredune development. *Earth Surface Processes and Landforms*, *26*(11), 1161–1176. https://doi.org/10.1002/esp.257

Argyilan, E. P., Forman, S. L., & Thompson, T. A. (2010). Variability of Lake Michigan water level during the past 1000 years reconstructed through optical dating of a coastal strandplain. *The Holocene*, *20*(5), 723–731. https://doi.org/10.1177/0959683609358913

Billy, J., Robin, N., Hein, C. J., Certain, R., & FitzGerald, D. M. (2014). Internal architecture of mixed sand-and-gravel beach ridges: Miquelon-Langlade Barrier, NW Atlantic. *Marine Geology*, *357*, 53–71. https://doi.org/10.1016/j.margeo.2014.07.011

Billy, J., Robin, N., Hein, C. J., Certain, R., & FitzGerald, D. M. (2015). Insight into the late Holocene sea-level changes in the NW Atlantic from a paraglacial beach-ridge plain south of Newfoundland. *Geomorphology*, *248*, 134–146.

Boon, J. D., & Mitchell, M. (2015). Nonlinear change in sea level observed at North American tide stations. *Journal of Coastal Research*, *31*(6), 1295–1305.

Bristow, C. S., & Pucillo, K. (2006). Quantifying rates of coastal progradation from sediment volume using GPR and OSL: The Holocene fill of Guichen Bay, south-east South Australia. *Sedimentology*, *53*(4), 769–788. https://doi.org/10.1111/j.1365-3091.2006.00792.x

Brooke, B., Lee, R., Cox, M., Olley, J., & Pietsch, T. (2008). Rates of shoreline progradation during the last 1700 years at Beachmere, Southeastern Queensland, Australia, based on optically stimulated luminescence dating of beach ridges. *Journal of Coastal Research*, 640–648.

Buynevich, I. V., FitzGerald, D. M., & van Heteren, S. (2004). Sedimentary records of intense storms in Holocene barrier sequences, Maine, USA. *Marine Geology*, *210*(1-4), 135–148. https://doi.org/10.1016/j.margeo.2004.05.007

Choi, K. H., Choi, J. H., & Kim, J. W. (2014). Reconstruction of Holocene coastal progradation on the east coast of Korea based on OSL dating and GPR surveys of beach-foredune ridges. *The Holocene*, *24*(1), 24–34. https://doi.org/10.1177/0959683613515728

Cohn, N., Hoonhout, B. M., Goldstein, E. B., De Vries, S., Moore, L. J., Durán Vinent, O., & Ruggiero, P. (2019). Exploring marine and aeolian controls on coastal foredune growth using a coupled numerical model. *Journal of Marine Science and Engineering*, *7*(1), 13. https://doi.org/10.3390/jmse7010013

Costas, S., Ferreira, Ó., Plomaritis, T. A., & Leorri, E. (2016). Coastal barrier stratigraphy for Holocene high-resolution sea-level reconstruction. *Scientific Reports*, *6*(1), 38726. https://doi.org/10.1038/srep38726

Davidson-Arnott, R. G., Hesp, P., Ollerhead, J., Walker, I., Bauer, B., Delgado-Fernandez, I., & Smyth, T. (2018). Sediment budget controls on foredune height: Comparing simulation model results with field data. *Earth Surface Processes and Landforms*, *43*(9), 1798–1810. https://doi.org/10.1002/esp.4354

Deaton, C. D., Hein, C. J., & Kirwan, M. L. (2017). Barrier island migration dominates ecogeomorphic feedbacks and drives salt marsh loss along the Virginia Atlantic Coast, USA. *Geology*, *45*(2), 123–126. https://doi.org/10.1130/G38459.1

Dougherty, A. J., Choi, J. H., & Dosseto, A. (2016). Prograded barriers+ GPR+ OSL = insight on coastal change over intermediate spatial and temporal scales. *Journal of Coastal Research*, *75*(sp1), 368–372. https://doi.org/10.2112/SI75-074.1

Engelhart, S. E., & Horton, B. P. (2012). Holocene sea level database for the Atlantic coast of the United States. *Quaternary Science Reviews*, *54*, 12–25. https://doi.org/10.1016/j.quascirev.2011.09.013

Fenster, M. S., Dolan, R., & Smith, J. J. (2016). Grain-size distributions and coastal morphodynamics along the southern Maryland and Virginia barrier islands. *Sedimentology*, *63*(4), 809–823. https://doi.org/10.1111/sed.12239

Finkelstein, K. (1983). Cape formation as a cause of erosion on adjacent shorelines. In *Coastal Zone'83* (pp. 620–640). New York: ASCE.

FitzGerald, D. M. (1982). Sediment bypassing at mixed energy tidal inlets. In *Coastal Engineering 1982* (pp. 1094–1118). Cape Town, South Africa: ASCE.

FitzGerald, D. M. (1984). Interactions between the ebb-tidal delta and landward shoreline: Price Inlet, South Carolina. *Journal of Sedimentary Research*, *54*(4).

French, J., Payo, A., Murray, B., Orford, J., Eliot, M., & Cowell, P. (2016). Appropriate complexity for the prediction of coastal and estuarine geomorphic behaviour at decadal to centennial scales. *Geomorphology*, *256*, 3–16. https://doi.org/10.1016/j.geomorph.2015.10.005

Guadiano, D. J., & Kana, T. W. (2001). Shoal bypassing in mixed energy inlets: Geomorphic variables and empirical predictions for nine South Carolina inlets. *Journal of Coastal Research*, *17*, 280–291.

Hails, J. R. (1968). The late Quaternary history of part of the mid-north coast, New South Wales, Australia. *Transactions of the Institute of British Geographers*, (44), 133–149. https://doi.org/10.2307/621753

Halsey, S. D., (1978). Late Quaternary geologic history and morphologic development of the barrier island system along the Delmarva Peninsula of the mid-Atlantic Bight (Dissertation). Newark, Delaware: University of Delaware, 592 pp.

Headland, J. R., Vallianos, L., & Sheldon, J. G. (1987). Coastal processes at Wallops Island, Virginia. In *Proceedings, Coastal Sediments'87, New Orleans, Louisiana, 12–14 May 1987* (pp. 1305–1320). New York: American Society of Civil Engineers.

Hede, M. U., Bendixen, M., Clemmensen, L. B., Kroon, A., & Nielsen, L. (2013). Joint interpretation of beach-ridge architecture and coastal topography show the validity of sea-level markers observed in ground-penetrating radar data. *The Holocene*, *23*(9), 1238–1246. https://doi.org/10.1177/0959683613484618

Hein, C. J., FitzGerald, D. M., Cleary, W. J., Albernaz, M. B., de Menezes, J. T., & Klein, A. H. D. F. (2013). Evidence for a transgressive barrier within a regressive strandplain system: Implications for complex coastal response to environmental change. *Sedimentology*, *60*(2), 469–502.

Hein, C. J., FitzGerald, D. M., Cleary, W. J., Albernaz, M. B., de Menezes, J. T., & Klein, A. H. D. F. (2013). Evidence for a transgressive barrier within a regressive strandplain system: Implications for complex coastal response to environmental change. *Sedimentology*, *60*(2), 469–502.

Hein, C. J., FitzGerald, D. M., de Souza, L. H., Georgiou, I. Y., Buynevich, I. V., Klein, A. H. D. F., et al. (2016). Complex coastal change in response to autogenic basin infilling: An example from a sub-tropical Holocene strandplain. *Sedimentology*, *63*(6), 1362–1395. https://doi.org/10.1111/sed.12265

Hein, C. J., Shawler, J. L., De Camargo, J. M., Klein, A. H. D. F., Tenebruso, C., & Fenster, M. S. (2019). The role of coastal sediment sinks in modifying longshore sand fluxes: examples from the coasts of southern Brazil and the mid-Atlantic, USA. In *The Proceedings of the Coastal Sediments 2019*. San Diego, USA: World Scientific Pub Co Inc.

Hesp, P. (2011). Dune Coasts. In E. Wolanski, & D. S. McLusky (Eds.), *Treatise on estuarine and coastal science* (Vol. 3, pp. 193–221). Waltham: Academic Press. https://doi.org/10.1016/B978-0-12-374711-2.00310-7

Himmelstoss, E. A., Kratzmann, M. G., & Thieler, E. R. (2017). National assessment of shoreline change—Summary statistics for updated vector shorelines and associated shoreline change data for the Gulf of Mexico and Southeast Atlantic coasts: U.S. Geological Survey Open-File Report 2017–1015, 8 p.

Johnson, D. W. (1919). *Shore processes and shoreline development*. NewYork, NY: John Wiley.

Kraus, N. C., & Hayashi, K. (2005). Numerical morphologic model of barrier island breaching. In *Coastal Engineering 2004: (In 4 Volumes)* (pp. 2120–2132). Lisbon, Portugal: World Scientific Press

Long, A. J., Strzelecki, M. C., Lloyd, J. M., & Bryant, C. L. (2012). Dating high Arctic Holocene relative sea level changes using juvenile articulated marine shells in raised beaches. *Quaternary Science Reviews*, *48*, 61–66. https://doi.org/10.1016/j.quascirev.2012.06.009

Mason, O. K. (1993). The geoarchaeology of beach ridges and cheniers: Studies of coastal evolution using archaeological data. *Journal of Coastal Research*, *9*(1), 126–146.

McBride, R. A., Fenster, M. S., Seminack, C. T., Richardson, T. M., Sepanik, J. M., Hanley, J. T., et al. (2015). Holocene barrier-island geology and morphodynamics of the Maryland and Virginia open-ocean coasts: Fenwick, Assateague, Chincoteague, Wallops, Cedar, and Parramore Islands. In D. K. Brezinski, J. P. Halka, & R. A. Ortt, Jr. (Eds.), *Tripping from the Fall Line: Field excursions for the GSA annual meeting*, (Vol. *40*, pp. 309–424). Baltimore: Geological Society of America Field Guide.

Moffatt and Nichol, Engineers (1986). Wallops Island shore protection study: NASA/Goddard Space Flight Facility, Wallops Island, Virginia, 86 p. with appendices.

National Park Service (2016). Digital pre-Hurricane Sandy geomorphological-GIS map of the Gateway National Recreation Area: Sandy Hook, Jamaica Bay and Staten Island Units, New Jersey and New York (NPS, GRD, GRI, GATE, GATE digital map) adapted from a Rutgers University Institute of Marine and Coastal Sciences unpublished digital data by Psuty, N.P., McLoughlin, S.M., Schmelz, W. and Spahn, A. (2014). *NPS Geologic Resources Inventory Program*. https://irma.nps.gov/DataStore/Reference/Profile/2233886

NOAA (2017). Method description: Detailed method for mapping sea level rise marsh migration. NOAA Office for Coastal Management, January, 2017. https://coast.noaa.gov/data/digitalcoast/pdf/slr-marsh-migration-methods.pdf

Nooren, K., Hoek, W. Z., Winkels, T., Huizinga, A., Van der Plicht, H., Van Dam, R. L., et al. (2017). The Usumacinta–Grijalva beach-ridge plain in southern Mexico: A high-resolution archive of river discharge and precipitation. *Earth Surface Dynamics*, *5*(3), 529–556. https://doi.org/10.5194/esurf-5-529-2017

Oliver, T. S., Donaldson, P., Sharples, C., Roach, M., & Woodroffe, C. D. (2017). Punctuated progradation of the Seven Mile Beach Holocene barrier system, southeastern Tasmania. *Marine Geology*, *386*, 76–87. https://doi.org/10.1016/j.margeo.2017.02.014

Oliver, T. S., Dougherty, A. J., Gliganic, L. A., & Woodroffe, C. D. (2015). Towards more robust chronologies of coastal progradation: Optically stimulated luminescence ages for the coastal plain at Moruya, south-eastern Australia. *The Holocene*, *25*(3), 536–546. https://doi.org/10.1177/0959683614561886

Oliver, T. S., Tamura, T., Short, A. D., & Woodroffe, C. D. (2018). Rapid shoreline progradation followed by vertical foredune building at Pedro Beach, southeastern Australia. *Earth Surface Processes and Landforms*, *44*, 655–666.

Oliver, T. S. N., Tamura, T., Hudson, J. P., & Woodroffe, C. D. (2017). Integrating millennial and interdecadal shoreline changes: Morpho-sedimentary investigation of two prograded barriers in southeastern Australia. *Geomorphology*, *288*, 129–147. https://doi.org/10.1016/j.geomorph.2017.03.019

Otvos, E. G. (2000). Beach ridges—Definitions and significance. *Geomorphology*, *32*(1-2), 83–108. https://doi.org/10.1016/S0169-555X(99)00075-6

Psuty, N. P. (1965). Beach-ridge development in Tabasco, Mexico 1. *Annals of the Association of American Geographers*, *55*(1), 112–124. https://doi.org/10.1111/j.1467-8306.1965.tb00509.x

Psuty, N. P. (2004). The coastal foredune: A morphological basis for regional coastal dune development. In M. Martinez, & N. P. Psuty (Eds.), *Coastal dunes: Ecology and conservation* (pp. 11–27). Berlin: Springer-Verlag.

Pye, K., & Blott, S. J. (2016). Assessment of beach and dune erosion and accretion using lidar: Impact of the stormy 2013–14 winter and longer term trends on the Sefton Coast, UK. *Geomorphology*, *266*, 146–167. https://doi.org/10.1016/j.geomorph.2016.05.011

Raff, J. L., Shawler, J. L., Ciarletta, D. J., Hein, E. A., Lorenzo-Trueba, J., & Hein, C. J. (2018). Insights into barrier-island stability derived from transgressive/regressive state changes of Parramore Island, Virginia. *Marine Geology*, *403*, 1–19. https://doi.org/10.1016/j.margeo.2018.04.007

Rhodes, E. G. (1980). Modes of Holocene coastal progradation: Gulf of Carpentaria (Thesis). Australian National University, Canberra.

Rice, T. E., Niedoroda, A. W., & Pratt, A. P. (1976). The coastal processes and geology: Virginia Barrier Islands. In *Ecosystem description: Virginia Coast reserve study* (pp. 107–384). Arlington, VA, USA: The Nature Conservancy.

Rink, W. J., & Forrest, B. (2005). Dating evidence for the accretion history of beach ridges on Cape Canaveral and Merritt Island, Florida, USA. *Journal of Coastal Research*, *215*, 1000–1008. https://doi.org/10.2112/03-0058.1

Roy, P. S., Cowell, P. J., Ferland, M. A., & Thom, B. G. (1994). Wave dominated coasts. In R. W. G. Carter, & C. D. Woodroffe (Eds.), *Coastal evolution: Late Quaternary shoreline morphodynamics* (pp. 121–186). Cambridge: Cambridge University Press.

Ruggiero, P., Hacker, S., Seabloom, E., & Zarnetske, P. (2018). The role of vegetation in determining dune morphology, exposure to sea-level rise, and storm-induced coastal hazards: A US Pacific Northwest perspective. In *Barrier dynamics and response to changing climate* (pp. 337–361). Cham: Springer. https://doi.org/10.1007/978-3-319-68086-6_11

Saye, S. E., Van der Wal, D., Pye, K., & Blott, S. J. (2005). Beach–dune morphological relationships and erosion/accretion: An investigation at five sites in England and Wales using lidar data. *Geomorphology*, *72*(1-4), 128–155. https://doi.org/10.1016/j.geomorph.2005.05.007

Seminack, C. T., & McBride, R. A. (2015). Geomorphic history and diagnostic features of former tidal inlets along Assateague Island, Maryland-Virginia: A life-cycle model for inlets along a wave dominated barrier islands. *Shore and Beach*, *83*, 3–24.

Smith, E. R., Reed, J. C., & Delwiche, I. L. (2016). *The Atlantic Coast of Maryland, sediment budget update: Tier 2, Assateague Island and Ocean City Inlet*. ERDC/CHL CHETN-XIV-48. Vicksburg, MS, USA.: US Army Engineer Research and Development Center.

Tamura, T. (2012). Beach ridges and prograded beach deposits as palaeoenvironment records. *Earth-Science Reviews*, *114*(3-4), 279–297. https://doi.org/10.1016/j.earscirev.2012.06.004

Vinent, O. D., & Moore, L. J. (2013). Vegetation controls on the maximum size of coastal dunes. *Proceedings of the National Academy of Sciences*, *110*(43), 17,217–17,222.

Walker, I. J., Davidson-Arnott, R. G., Bauer, B. O., Hesp, P. A., Delgado-Fernandez, I., Ollerhead, J., & Smyth, T. A. (2017). Scale-dependent perspectives on the geomorphology and evolution of beach-dune systems. *Earth-Science Reviews*, *171*, 220–253. https://doi.org/10.1016/j.earscirev.2017.04.011

Young, A. P., & Ashford, S. A. (2006). Application of airborne lidar for seacliff volumetric change and beach-sediment budget contributions. *Journal of Coastal Research*, *222*, 307–318. https://doi.org/10.2112/05-0548.1

References From the Supporting Information

Davidson-Arnott, R. G., & Law, M. N. (1996). Measurement and prediction of long-term sediment supply to coastal foredunes. *Journal of Coastal Research*, 654–663.

Del Angel, D. (2012). Dune-beach morphodynamic interaction along a semi-arid, wave dominated barrier island: South Padre Island, Texas (Dissertation). Texas A&M University–Corpus Christi, TX, USA.

De Vries, S., Southgate, H. N., Kanning, W., & Ranasinghe, R. (2012). Dune behavior and aeolian transport on decadal timescales. *Coastal Engineering*, *67*, 41–53. https://doi.org/10.1016/j.coastaleng.2012.04.002

Hoonhout, B., & de Vries, S. (2017). Aeolian sediment supply at a mega nourishment. *Coastal Engineering*, *123*, 11–20. https://doi.org/10.1016/j.coastaleng.2017.03.001

Kaczkowski, H. L., Kana, T. W., Traynum, S. B., & Visser, R. (2017). Beach-fill equilibration and dune growth at two large-scale nourishment sites. *Ocean Dynamics*, *68*(9), 1191–1206.

NOAA (2018). Wachapreague, Virginia—Station ID: 8631044. *NOAA Tides and Currents*. https://tidesandcurrents.noaa.gov/stationhome.html?id=8631044

Ruggiero, P., Mull, J., Zarnetske, P., Hacker, S., & Seabloom, E. (2011). Interannual to decadal foredune evolution. In *The Proceedings of the Coastal Sediments 2011: In 3 Volumes* (pp. 698–711). Miami, FA: World Scientific Press.